Geophys. J. Int. (2004) **156,** 39–44 doi: 10.1111/j.1365-246X.2004.02040.x

FAST TRACK PAPER

The scatter of time-delays in shear-wave splitting above small earthquakes

Stuart Crampin,[1,*] Sheila Peacock,[2] Yuan Gao[1,†] and Sebastien Chastin[1]

[1] *Shear-Wave Analysis Group, School of GeoSciences, University of Edinburgh, Grant Institute, King's Buildings, West Mains Road, Edinburgh* EH9 3JW, *UK. E-mails: scrampin@ed.ac.uk; ygao@staffmail.ed.ac.uk; schastin@glg.ed.ac.uk*

[2] *School of Earth Sciences, University of Birmingham, Edgbaston, Birmingham* B15 2TT, *England UK. E-mail: peacocks@es4.ers.bham.ac.uk*

Accepted 2003 May 13. Received 2003 April 7; in original form 2002 October 9

SUMMARY

Measurements of time-delays in seismic shear-wave splitting above small earthquakes typically display a scatter of often as much as ±80 per cent about the mean. Changes in the average time-delay appear to be related to changes of stress, but applications of this potentially powerful tool have been handicapped by the previously inexplicable scatter in time-delays above earthquakes. In contrast, measurements of shear-wave time-delays in controlled-source exploration seismics are typically well controlled and display little scatter. Previous estimates of possible causes of scatter cannot produce sufficient variation specifically above earthquakes. Here we show that 90°-flips in shear-wave polarizations due to fluctuating high pore-fluid pressures on seismically-active fault planes are the most likely cause of the scatter.

Key words: crack-critical systems, critically-high pore-fluid pressures, scatter in time-delays, shear-wave splitting, 90°-flips.

GJI Seismology

1 INTRODUCTION

Stress-aligned shear-wave splitting (seismic birefringence), caused by propagation through fluid-saturated microcracks, is widely observed in almost all *in situ* rocks in the crust (Crampin 1994, 1996; Winterstein 1996). Theoretically, anisotropic poro-elasticity (APE) models rock mass deformation with the fundamental assumption that the cracks in the crust are so closely spaced that they form a critical system (Zatsepin & Crampin 1997; Crampin & Zatsepin 1997). The APE mechanism is fluid movement by flow or diffusion along pressure gradients between neighbouring fluid-saturated grain-boundary cracks, and low aspect-ratio pores and pore throats, at different orientations to the stress-field. APE shows that the parameters that control low-level (pre-fracturing) deformation also control shear-wave splitting. Consequently, fluctuations in time-delays between the split shear-waves can directly monitor stress-induced changes to microcrack geometry. As a result, changes in the average time-delay above small earthquakes led to a correct estimate of the time and magnitude of an $M = 5$ earthquake in SW Iceland (Crampin *et al.* 1999). This estimate was in a comparatively narrow window, where local knowledge also recognized the fault that moved. Consequently, we claim the stress-forecast was successful. However, the problem with using earthquakes as the source of shear-waves is the enormous scatter in measured time-delays, which are often observed to be ±80 per cent about the mean.

In contrast, shear-wave splitting in controlled-source exploration seismology is well behaved and shows little scatter (Li *et al.* 1993; Yardley & Crampin 1993). APE has been accurately calibrated in two controlled-source experiments by Angerer *et al.* (2002), who calculated ('predicted with hindsight') the response of a fractured hydrocarbon reservoir to two different CO_2-injections. The difference in scatter between shear-wave splitting above small earthquakes (up to ±80 per cent about the mean) and controlled-source observations (very little scatter) has been an unresolved problem that cast doubts on all interpretations of shear-wave splitting. We need to seek an explanation for the scatter that only applies to shear-wave splitting above small earthquakes.

The scatter at ±80 per cent from similar earthquakes with similar ray paths is just too large to be explained by conventional geophysical sources of scatter (Volti & Crampin 2003a). The solution presented here, based on new observations and modelling of shear-wave splitting, is that high pore-fluid pressures surrounding seismically-active fault planes cause 90°-flips where the faster and slower split shear-waves exchange polarizations. We show that variations in 90°-flips could be caused by comparatively minor temporal variations in stress and pressure changes as stress is released at every earthquake. This could easily lead to the observed ±80 per cent scatter in time-delays and thus help to resolve this long-standing problem.

*Also at: Edinburgh Anisotropy Project, British Geological Survey, Murchison House, West Mains Road, Edinburgh EH9 3LA, UK. http://www.glg.ed.ac.uk/∼scrampin/opinion/

†Now at: Centre for Analysis and Prediction, China Seismological Bureau, Beijing 100036, China. E-mail: gaoyuan@seis.ac.cn

2 SHEAR-WAVE SPLITTING AND THE SCATTER OF TIME-DELAYS

Shear-wave splitting due to the azimuthal anisotropy of stress-aligned fluid-saturated microcracks is observed for propagation through almost all sedimentary, igneous, and metamorphic rocks. APE modelling approximately matches a large range of phenomena pertaining to cracks, shear-waves, and stress (Crampin 1999). The match is almost exact in those few cases where crack parameters *in situ* can be independently measured (Crampin & Zatsepin 1997; Angerer *et al.* 2002). Usually however, rocks at depth are subject to such high pressures and temperatures that any approach to or recovery of *in situ* rock destroys the microcrack structure through the stress-, temperature-, and pressure-induced trauma of drilling. This means that seismic propagation techniques are the one of the few ways to examine *in situ* cracks.

Fig. 1 shows measurements of shear-wave splitting time-delays at a station in Iceland using small earthquakes as the shear-wave source (Volti & Crampin 2003b). The substantial scatter is remarkably similar to that seen elsewhere in Iceland and at two places on the San Andreas Fault in California (reviewed by Crampin 1999). Table 1 summarizes the observed scatter of time-delays. The only places where measurements of shear-wave time-delays above small earthquakes have not shown such a large scatter is when the recordings have been made above isolated swarms of earthquakes (Booth *et al.* 1990; Gao *et al.* 1998). Isolated swarms have small source volumes (typically 1 or 2 km in diameter), where earthquakes have repeatable source parameters (Crampin 1993). Consequently, it may not be surprising that measurements of time-delays above isolated swarms do not show the typical large scatter. However, both observations of shear-wave time-delays above isolated swarms have sparse data sets and the scatter could be under-estimated.

3 PREVIOUS EXPLANATIONS OF THE SCATTER IN TIME-DELAYS

Table 2 lists different sources of scatter based on a conventional non-critical geophysics. These mechanisms are more fully discussed in Volti & Crampin (2003a). Table 2 also lists comparatively generous estimates (in light of listed comments) of the amounts of scatter. Each mechanism could, and probably does, induce a small percentage of scatter, but the mechanisms are not correlated and in combination could not produce the consistent ±80 per cent scatter actually observed. If the mechanisms in Table 2 caused the whole scatter, repetitions of similar earthquakes in similar locations would be expected to induce similar scatter and this is not observed. For example, in Iceland, where there is comparatively frequent localized swarm activity with many events in a limited time from comparatively limited source volumes which, for sources of scatter in Table 2, might be expected to show similar time-delays. In fact, the time-delays from such swarms typically produce vertical 'stripes' of time-delays that span the whole range of scattered time-delays from previous observations. The foreshock and aftershock sequence of the $M = 5$ earthquake in 1998 November, in Fig. 1 shows one such

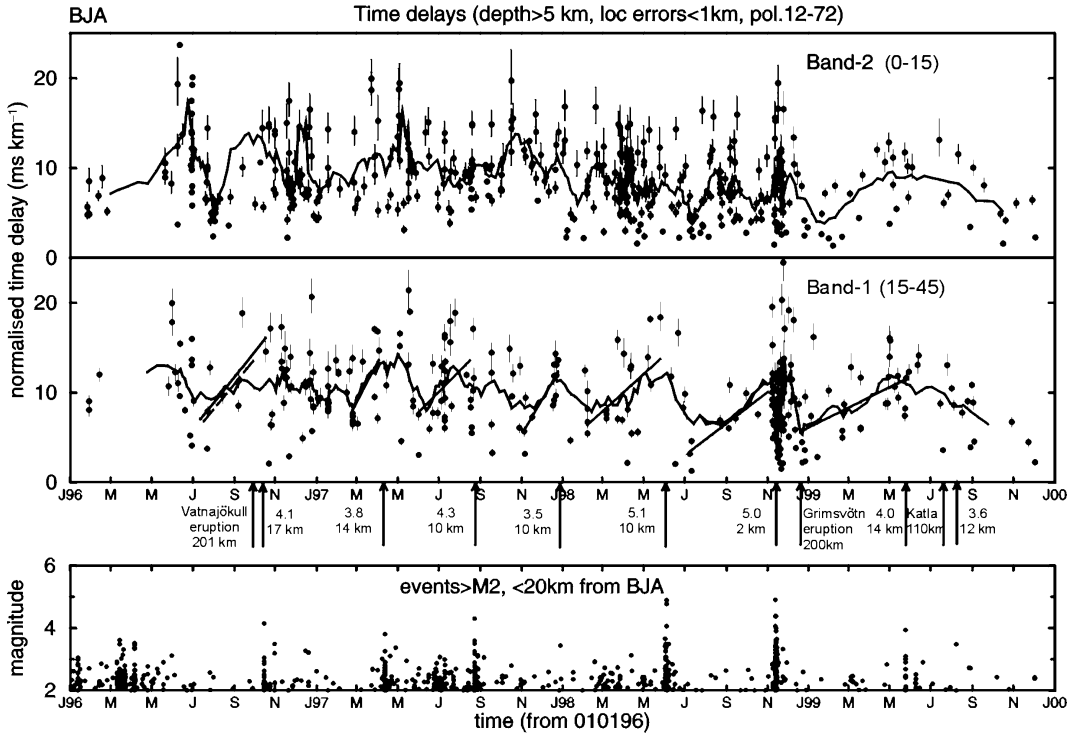

Figure 1. Typical example of scatter of time-delays in shear-wave splitting observed above small earthquakes. Time-delays from 1996 January 1 to 1999 December 31 at Station BJA in SW Iceland. Time-delays are normalized to a 1 km path length. Middle and upper diagrams show variations for ray path directions in Band-1, and Band-2. Band-1 is the double-leafed solid angle of ray paths making angles between 15° to 45° either side of the average parallel vertical crack plane. Band-2 is the solid angle within 15° of the average crack plane (Crampin 1999). Ray paths in Band-1 are sensitive to crack aspect-ratio and hence to stress changes, whereas Band-2 is sensitive to crack density (Crampin 1999). The straight lines in Band-1 are least-squares estimates beginning just before a minimum of the nine-point moving average and ending at a larger earthquake or eruption. The dashed line refers to changes before the Vatnajökull eruption. The arrows below each plot indicate the times of these larger events with estimated magnitudes and epicentral distances. The bottom diagram shows the magnitudes of earthquakes greater than $M = 2$ within 20 km of BJA (After Crampin 1999; Volti & Crampin 2003b).

Table 1. Summary of presence or absence of scatter in time-delays in shear-wave splitting.

*Substantial scatter of up to ±80 per cent observed above small earthquakes**
At Station KNW before and after the $M = 6$ 1986 North Palm Springs Earthquake on the San Andreas Fault, California[1,2]
At several stations of the (HRSN) Parkfield Network before and after a $M_L = 4$ earthquake on the San Andreas Fault, California[3]
At four stations in Iceland before and after some five earthquakes ($3.8 \leq M \leq 5.1$) and several volcanic eruptions[4]
Much smaller scatter above isolated swarms[5] *of small earthquakes*†*
At several stations above an isolated swarm in Arkansas[6]
Two stations above an isolated swarm in Hainan Island, China[7]
Negligible scatter in controlled-source vertical-seismic-profiles and seismic reflection surveys‡
Detailed VSP survey[8]
Range of seismic reflection surveys[9]
Reflection surveys responding to two CO_2-injections[10]

[1]Peacock *et al.* (1988); [2]Crampin *et al.* (1990, 1991); [3]Liu *et al.* (1997); [4]Volti & Crampin (2003b); [5]Crampin (1993); [6]Booth *et al.* (1990); [7]Gao *et al.* (1998); [8]Yardley & Crampin (1993); [9]Li *et al.* (1993); [10]Angerer *et al.* (2002).
*Time-delays have only been studied for temporal variations before earthquakes.
†Both examples listed have sparse data sets and scatter could be under-estimated.
‡There are many examples of controlled-source seismograms showing negligible scatter.

Table 2. Possible causes of scatter in time-delays above small earthquakes assuming a conventional (non-critical) crust and estimated scatter (after Volti & Crampin 2003a).

Possible cause	Comments	Estimated scatter
Geological and geophysical complications and heterogeneities		
Complicated geology beneath seismic stations	Theory[1] and observations[2,3,4] suggest that shear-wave splitting is sensitive to stress and insensitive to geological structure. If geological complications were the cause, different complications would be expected beneath each station, but the degree of scatter is remarkably similar above all earthquakes	±10 per cent
Complicated stress-aligned cracking beneath stations	As above	±10 per cent
Errors in earthquake locations and seismogram measurement		
Time-delays normalized will show irregularities if focal locations are in error	The errors in path length for earthquakes within the shear-wave window are usually too small to cause the substantial scatter[2,3]	±20 per cent
Time-delays along different ray paths from different source locations may show scatter	Improved locations[3,5] do not result in reduced time-delay variations[3]	±10 per cent
Errors in picking time-delays	Time-delays are checked and all doubtful estimates are rejected, so that large errors are believed to be uncommon	±10 per cent
Different focal mechanisms		
Small variations in source radiation can produce significant different polarizations and hence different time-delay images	Observed polarization directions are comparatively uniform[2,3] so large differences in time-delays are unlikely	±10 per cent
Complications in anisotropic propagation		
3-D variations inherent in time-delay geometry expect time-delays to vary from zero to maximum values in Band-1 directions[2]	Such variations are different in Band-1 and Band-2[2,3], yet amplitude of scatter in both Bands is observed to be similar[2,3]	±5 per cent
Variations in Band-1 are close to line singularities[6] and *may* be close to point singularities[2,6] which could seriously disturb time-delays	Presence or absence of singularities are markedly different in Band-1 and Band-2[2], yet scatter is observed to be similar[3]	±5 per cent

[1]Zatsepin & Crampin (1997); [2]Crampin (1994, 1996, 1999); [3]Volti & Crampin (2003b); [4]Winterstein (1996); [5]Slunga *et al.* (1995); [6]Crampin & Yedlin (1981).

stripe of time-delays spanning the previous scatter. This suggests that small changes in earthquake location and/or ray path can reproduce almost the whole range of scattered values. This is difficult to explain by conventional wave propagation through heterogeneous elastic-solid geometries.

4 OBSERVATIONS OF 90°-FLIPS IN SHEAR-WAVE POLARIZATIONS

Although the phenomenon of 90°-flips had not been recognized at that time, the first observations of 90°-flips above small earthquakes are probably the shear-wave polarizations observed at Station KNW, of the Anza Seismic Network (Peacock *et al.* 1988; Crampin *et al.* 1990, 1991). KNW was within 3 km of the Hot Springs Fault branch of the San Jacinto Fault, part of the San Andreas Fault system. Liu *et al.* (1997) positively identified 90°-flips at Station MM, of the Parkfield Seismic Network, sited immediately above the San Andreas Fault.

The presence of 90°-flips in controlled-source seismics was first positively identified in a vertical seismic profile in the Caucasus Oil Field where shear-wave splitting time-delays, after an initial increase, decreased as they penetrated into an overpressurized

reservoir (Crampin *et al.* 1996; Slater 1997). The decrease indicated a 90°-flip in the polarization of the faster split shear-wave. Angerer *et al.* (2002), in the best calibration of APE to date, calculated (predicted with 'hindsight') the response of a fractured reservoir to two injections at different CO_2-pressures. One of the pressures was close to the maximum horizontal stress and caused 90°-flips in shear-wave splitting.

The new data are observations of shear-wave splitting in Iceland (Crampin *et al.* 2000). The polarizations at most stations are aligned approximately NE to SW in what appears to be the direction of maximum horizontal stress. The only exceptions are the polarizations at three new stations sited within 3 km of the surface break of the Húsavík-Flatey Fault, a major transform fault of the Tjörnes Fracture Zone of the Mid-Atlantic Ridge. The stations were installed as part of the EC funded SMSITES Project (Crampin *et al.* 2000) specifically to seek 90°-flips. The shear-wave polarizations at these new stations are fault parallel and approximately orthogonal to the polarizations observed elsewhere in Iceland. The change in polarizations is interpreted as 90°-flips in shear-wave polarizations caused by high pore-fluid pressures surrounding the seismically-active fault plane.

Crampin *et al.* (2000) theoretically model these 90°-flips with APE. They show that the shear-wave polarizations will display approximately orthogonal orientations (90°-flips) when the pore-fluid pressures permeating the fluid-saturated microcracks are within one or two MPa of the maximum horizontal stress: a level when fracturing (and hydraulic fracturing) necessarily occur. The physical mechanism for 90°-flips is that microcrack distribution geometry is rearranged by opening and closing fluid-saturated microcracks by varying pore pressures. Specifically, lowering effective stress allows cracks not parallel to the direction of maximum compression to open, and increasing pore pressure widens cracks parallel to maximum compression. The previous stress-parallel polarizations for near-vertical propagation of faster split shear-waves are changed (by 90°-flips) and become perpendicular to the previous directions (Crampin *et al.* 2000).

5 VARYING CRITICAL PRESSURES

Fig. 2 shows the effect of increasing pore-fluid pressure in fluid-saturated cracks under ten different stress regimes (the mechanism is discussed by Crampin *et al.* 2000). When an earthquake occurs in critically-pressurized rocks, at EQ for example, stress is released, and the figure indicates several simple possibilities. There may be a decrease in pressure under the same triaxial stress field, to point A for example. More generally, there may be a release of stress and a release of pore-fluid pressure, leading to different points B, C, or D, for example, in different stress and pressure regimes. The new conditions at A to D may evolve to further seismicity in associated stress and pressure environments. In particular, note that subcritical pore-fluid pressures at one state of triaxial stress may still be close to criticality at lower, pre-earthquake, stress states.

The stress-release by real earthquakes will be complicated, but Fig. 2 indicates that the triaxial stress-field, and pore-fluid pressure, surrounding the fault plane, necessarily change following each earthquake. The volume of critical pore-fluid pressure will change in size and shape, both during and following earthquakes. Consequently, ray paths from successive earthquakes even from similar locations will be from different stress and pressure regimes and will sample different segments of critically-pressurized rocks. Fig. 3 shows the effects of different proportions of pressurized rock on the time-delays of shear-wave splitting.

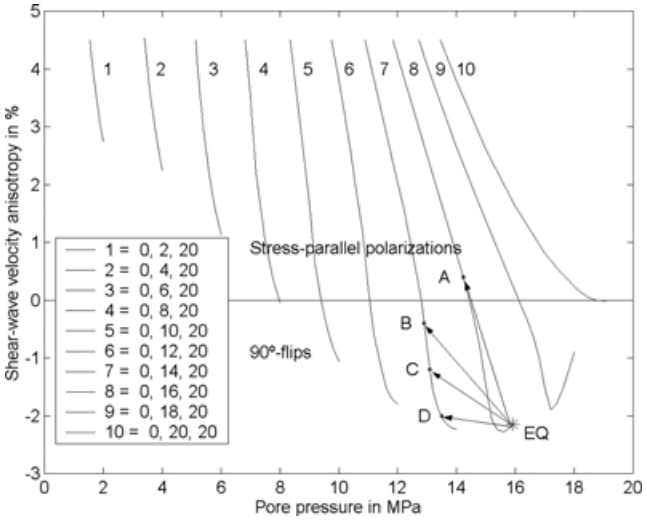

Figure 2. Variation of percentage shear-wave velocity anisotropy with increasing pore-fluid pressure for ten different sets of principal axes of stress showing 90°-flips in polarization as anisotropy becomes negative for pore-fluid pressures approaching s_H. The inset shows the ten different sets of principal axes of differential stress, s_h, s_H, and s_V in MPa, as discussed by Crampin *et al.* (2000). Following stress release by earthquake at EQ, stress and pressure changes to A, B, C, D, say, in different stress and pressure environments.

6 90°-FLIPS AS THE SOURCE OF TIME-DELAY SCATTER

Possible 90°-flips have been observed at the surface above earthquakes located only on major faults, the San Andreas and the Húsavík-Flatey. These faults cut a large part of the crust and extend to close to the surface. Crampin *et al.* (2000) show that on the Húsavík-Flatey Fault the 90°-flips persist for ray paths to the surface as far as 3 km from the surface break. Similar observations at Station GRI, some 10 km from earthquakes on the Grímsey Lineament in the same Tjörnes Fracture Zone, do not show 90°-flips. This places some limits on the penetration of high pressures away from major fault planes.

It is now well established that high pore-fluid pressures are necessary in seismically-active fault planes in order to reduce friction enough for slippage to occur and asperities overcome (Sibson 1981, 1990; Rice 1992; Hickman *et al.* 1995). We have shown the effects of high pressures on major faults (Crampin *et al.* 2000), we now examine the implications of high pore-fluid pressures on all smaller faults.

Fig. 3 shows a simplified model of the effects of different volumes (different path segments) of high pore-fluid pressure around a vertical fault, inducing 90°-flips along a vertical ray path from an earthquake at 10 km depth. The anisotropy of each 1 km of depth in Fig. 3(a) for vertically propagating waves is assumed to cause the same time-delay between split shear-wave arrivals of Δt (varying the degree of velocity anisotropy with depth would accentuate scatter). We assume time-delays are positive in low pressurized rocks, so that the faster split shear wave is polarized parallel to the cracks, and negative in critically-pressurized rocks when there are 90°-flips. When the whole ray path is at low (subcritical) fluid pressure, there is no critically pressurized rock, $a = 0$, and the length of the ray path through normal pressures is $b = 10$ km. The total time-delay at the surface will be $10 \times \Delta t$ leading to a normalized time-delay of Δt at the surface with a conventional stress-aligned polarization.

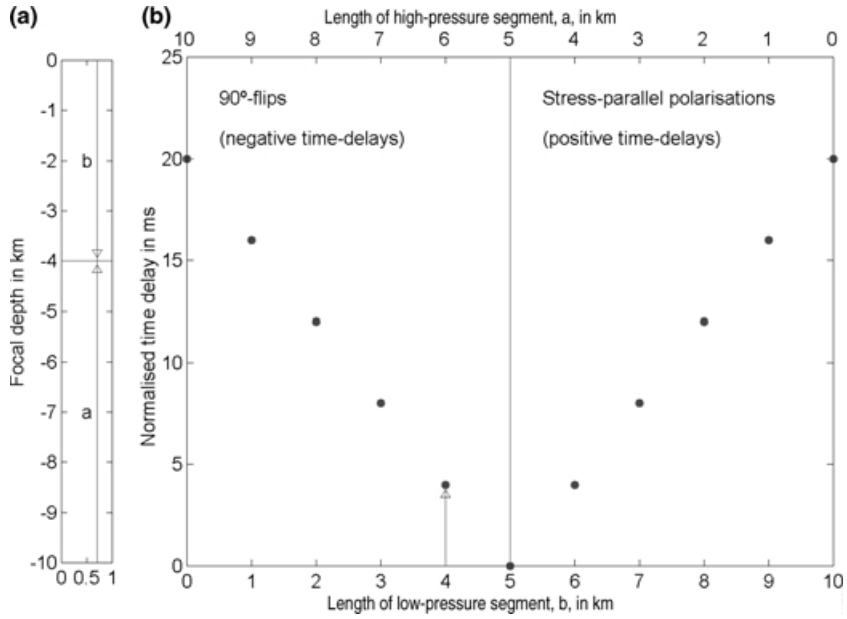

Figure 3. Variation of normalized time-delays at the surface for ten different lengths of critically-pressurized path segments, a, above an earthquake assumed to be at 10 km depth, where the normally-pressurized segment $b = 10 - a$. The critically-pressurized segment is assumed to be close to the seismically active fault plane. Example of high-pressure segment indicated at $a = 6$ km, $b = 4$ km.

For other distributions, the conventional stress-aligned normalized time-delay at the surface is $|(b - a) \times \Delta t|/10$, equivalent to:

$$|(10 - 2a) \times \Delta t|/10; \quad (1)$$

where $a = 10 - b$. Both conventional stress-aligned shear-wave splitting and 90°-flips give normalized time-delays from 0 (no time-delay) to Δt, depending on whether the high-pressure segment is less than or more than half the ray path.

In Fig. 3(b), Δt is taken as 20 ms, equivalent to the maximum normalized time-delay per kilometre commonly observed in Iceland (Volti & Crampin 2003b). The scatter indicated in Fig. 3(b) is for the same earthquake focal depth with varying lengths of critically pressurized path. It is approximately equivalent to the scatter observed in Iceland both in conventional stress-aligned shear-wave splitting and in 90°-flips. The scatter is caused by variations in the volume of rock containing high-pressure fluid around the hypothesized fault plane. For shear-waves from earthquakes on small fault planes where the high fluid-pressures extend for less than half the ray path, the split shear waves at the surface show scattered time-delays but have the conventional stress-aligned, crack-parallel, shear-wave polarizations generally observed (Crampin 1994).

For shear-wave signals from earthquakes on large fault planes, where the high fluid-pressures extend for more than half the ray path, although not necessarily to the free-surface, the time-delays show a similar scatter but are normalized from negative time-delays and the polarizations show 90°-flips. This reproduces the 90°-flips observed above the major San Andreas and Húsavík-Flatey Faults, where it is reasonable to assume that the high pressures associated with the large fault planes are present for over half the ray path.

7 CONCLUSIONS

We have shown that varying volumes of rock containing critically pressured fluids surrounding seismically-active fault planes can easily account for the large scatter in time-delays observed above small earthquakes. They account for the scatter both for conventional stress-aligned shear-wave splitting observed at the surface, and for splitting with 90°-flips in shear-wave polarizations observed near major faults that traverse most of the crust. The difference being where the critically pressurized path is less than, or more than, half the total ray path. As high pore-fluid pressures are expected on all seismically-active fault planes, and other mechanisms for scatter are likely to cause only small scatter, we conclude that the large observed scatter is principally caused by rapid temporal variations in high pore-fluid pressures and triaxial stress-fields following earthquakes on seismically-active fault planes.

Many rose diagrams of shear-wave polarizations above small earthquakes show a small proportion of polarizations orthogonal to the direction of maximum horizontal stress. In the past, these have usually been interpreted as the earthquake source radiating shear-waves with wholly second arrival polarizations so that the faster arrival is not excited and only the slower shear-wave propagates. Fig. 3 suggests that such orthogonal polarizations may also be caused by high fluid-pressures occasionally extending to more than half the ray path to the surface.

An interesting implication of Fig. 3 is that the highest value of the scattered time-delay is the actual value of the shear-wave splitting time-delay in ms for the *in situ* rock. It had previously been thought that the least-squares fits, of the lines in Fig. 1 for example, were approximating the actual shear-wave time-delays in *in situ* rock in ms. Fig. 3 suggests that the maximum value of normalized time-delay in the scatter, not the mean, may be close to the value of splitting in *in situ* rock.

We conclude that the scatter in time-delays above almost all small earthquakes is primarily caused by the fluctuations in the time and location of high pore-fluid pressures surrounding seismically-active fault planes causing varying proportions of 90°-flips in shear-wave polarizations along shear-wave ray paths.

This has several implications.

(1) The scatter above all earthquakes implies that all seismically-active faults however small are surrounded by high pore-fluid pressures, confirming the hypotheses of Sibson (1981, 1990), Rice (1992), Hickman *et al.* (1995), and others.

(2) It implies in particular that large earthquakes, involving slip on large fault planes, cannot take place unless there are high pore-fluid pressures surrounding the fault. This means that small earthquakes on such a fault plane will show 90°-flips, if the fault is preparing for a large earthquake. Earthquakes on the Húsavík-Flatey Fault show such 90°-flips. This implies that the fault is critically pressurized over most of its surface and hence there is the possibility of a large earthquake.

(3) It implies that monitoring the approach of fracture-criticality and earthquake occurrence by shear-wave splitting using small earthquakes as the shear-wave source will typically display a large scatter. This means that monitoring the approach of criticality with controlled source seismics, sufficiently far from active seismicity to avoid high pore-fluid pressures, can monitor the build-up of stress without the scatter introduced by 90°-flips. This suggests that the Stress-Monitoring Site geometry, where cross-hole seismics between deep boreholes monitors shear-wave splitting along the particular ray paths sensitive to increasing stress (Crampin 2001) avoiding high pore-fluid pressures is likely to be a more reliable measure of stress-induced changes than shear-waves from small earthquakes.

(4) The presence of high pore-fluid pressures around seismically-active faults is likely to be put to the test soon in the several attempts to drill into seismically-active faults. The evidence in this paper suggests that drilling engineers should be cautious when approaching such faults. However, high pressures do not necessarily mean large volumes of water, so that a mitigating factor for drilling may be that the high pressures might be momentary and not involve the ejection of large quantities of water. It will be interesting to find out.

ACKNOWLEDGMENTS

This work was partially supported by the European Commission SMSITES and PREPARED Projects, Contract Numbers EVR1-CT1999-40002 and EVG1-CT2002-00073, respectively. YG was supported partly by China MOST under Contracts 2001BA601B02 and NSFC Project 40274011, and partly by the UK Royal Society Fellowship Programme. We thank Sergei Zatsepin, Peter Leary, and partners of the SMSITES Project for numerous fruitful discussions, and we are grateful to David Taylor for the use of ANISEIS software.

REFERENCES

Angerer, E., Crampin, S., Li, X.-Y. & Davis, T.L., 2002. Processing, modelling, and predicting time-lapse effects of over-pressured fluid-injection in a fractured reservoir, *Geophys. J. Int.,* **149,** 267–280.

Booth, D.C., Crampin, S., Lovell, J.H. & Chiu, J.-M., 1990. Temporal changes in shear-wave splitting during an earthquake swarm in Arkansas, *J. geophys. Res.,* **95,** 11 151–11 164.

Crampin, S., 1993. Do you know of an isolated swarm of small earthquakes?, *EOS, Trans. Am. geophys. Un.,* **74,** 451, 460.

Crampin, S., 1994. The fracture criticality of crustal rocks, *Geophys. J. Int.,* **118,** 428–438.

Crampin, S., 1996. Anisotropists Digest 149 and 150, **1,** *anisotropists@sep.stanford.edu*.

Crampin, S., 1999. Calculable fluid-rock interactions, *J. Geol. Soc.,* **156,** 501–514.

Crampin, S., 2001. Developing stress-monitoring sites using cross-hole seismology to stress-forecast the times and magnitudes of future earthquakes, *Tectonophysics,* **338,** 233–245.

Crampin, S. & Yedlin, M., 1981. Shear-wave singularities of wave propagation in anisotropic media, *J. Geophys.,* **49,** 43–46.

Crampin, S. & Zatsepin, S.V., 1997. Modelling the compliance of crustal rock, II—response to temporal changes before earthquakes, *Geophys. J. Int.,* **129,** 495–506.

Crampin, S., Booth, D.C., Evans, R., Peacock, S. & Fletcher, J.B., 1990. Changes in shear wave splitting at Anza near the time of the North Palm Springs Earthquake, *J. geophys. Res.,* **95,** 11 197–11 212.

Crampin, S., Booth, D.C., Evans, R., Peacock, S. & Fletcher, J.B., 1991. Comment on 'Quantitative Measurements of Shear Wave Polarizations at the Anza Seismic Network, Southern California: Implications for Shear Wave Splitting and Earthquake Prediction', eds Aster, R.C., Shearer, P.M. & Berger, J., *J. geophys. Res.,* **96,** 6403–6414.

Crampin, S., Zatsepin, S.V., Slater, C. & Brodov, L.Y., 1996. Abnormal shear-wave polarizations as indicators of pressures and over pressures, *58th Conf., EAGE, Amsterdam, Extended Abstracts,* X038.

Crampin, S., Volti, T. & Stefánsson, R., 1999. A successfully stress-forecast earthquake, *Geophys. J. Int.,* **138,** F1–F5.

Crampin, S., Volti, T. & Jackson, P., 2000. Developing a stress-monitoring site (SMS) near Húsavík for stress-forecasting the times and magnitudes of future large earthquakes, in *Destructive Earthquakes: Understanding Crustal Processes Leading to Destructive Earthquakes. Proc. 2nd EU-Japan Workshop on Seismic Risk*, pp. 136–149, eds Thorkelsson, B. & Yeroyanni, M., June 23–27, 1999, Europ. Comm., Res. Dir. Gen.

Crampin, S., Volti, T., Chastin, S., Gudmundsson, A. & Stefánsson, R., 2002. Indication of high pore-fluid pressures in a seismically-active fault zone, *Geophys. J. Int.,* **151,** F1–F5.

Gao, Y., Wang, P., Zheng, S., Wang, M., Chen, Y. & Zhou, H., 1998. Temporal changes in shear-wave splitting at an isolated swarm of small earthquakes in 1992 near Dongfang, Hainan Island Southern China, *Geophys. J. Int.,* **135,** 102–112.

Hickman, S., Sibson, R.H. & Bruhn, R., 1995. Introduction to special section: mechanical involvement of fluids in faulting, *J. geophys. Res.,* **100,** 12 831–12 840.

Li, X.-Y., Mueller, M.C. & Crampin, S., 1993. Case studies of shear-wave splitting in reflection surveys in South Texas, *Can. J. Expl. Geophys.,* **29,** 189–215.

Liu, Y., Crampin, S. & Main, I., 1997. Shear-wave anisotropy: spatial and temporal variations in time delays at Parkfield, Central California, *Geophys. J. Int.,* **130,** 771–785.

Peacock, S., Crampin, S., Booth, D.C. & Fletcher, J.B., 1988. Shear-wave splitting in the Anza seismic gap, Southern California: temporal variations as possible precursors, *J. geophys. Res.,* **93,** 3339–3356.

Rice, J.R., 1992. Fault stress states, pore pressure distribution, and the weakness of the San Andreas fault, in Fault Mechanics and Transport Properties of Rocks, pp. 475–503, eds Evans, B. & Wong, T.-F., Academic Press, San Diego.

Sibson, R.H., 1981. Controls on low-stress hydro-fracture dilatancy in thrust, wrench and normal fault terrains, *Nature* **289,** 665–667.

Sibson, R.H., 1990. Rupture nucleation on unfavorably oriented faults, *Bull. seism. Soc. Am.,* **80,** 1580–1604.

Slater, C.P., 1997. Estimation and modelling of anisotropy in vertical and walkaway seismic profiles at two North Caucasus Oil Fields, *PhD dissertation,* University of Edinburgh, Edinburgh.

Slunga, R., Rögnvaldsson, S.Th. & Böðvarsson, R., 1995. Absolute and relative location of similar events with application to microearthquakes in Southern Iceland, *Geophys. J. Int.,* **123,** 409–419.

Volti, T. & Crampin, S., 2003a. A four-year study of shear-wave splitting in Iceland: 1—Background and preliminary analysis, in *New Insights into Structural Interpretation and Modelling*, Vol. 212, pp. 117–133, ed. Nieuwland, D.A., Geol. Soc., Spec. Publ., Geol. Soc., London.

Volti, T. & Crampin, S., 2003b. A four-year study of shear-wave splitting in Iceland: 2—Temporal changes before earthquakes and volcanic eruptions, in *New Insights into Structural Interpretation and Modelling*, Vo. 212, pp. 135–149, ed. Nieuwland, D.A., Geol. Soc., Spec. Publ., Geol. Soc., London.

Winterstein, D.L., 1996. Anisotropists Digest, **1,** 147, *anisotropists@sep.stanford.edu*.

Yardley, G.S. & Crampin, S., 1993. Shear-wave anisotropy in the Austin Chalk, Texas, from multi-offset VSP data: case studies, *Can. J. Expl. Geophys.,* **29,** 163–176.

Zatsepin, S.V. & Crampin, S., 1997. Modelling the compliance of crustal rock: I—response of shear-wave splitting to differential stress, *Geophys. J. Int.,* **129,** 477–494.